UDK 625.843:620.194
Original scientific article/Izvirni znanstveni članek

ISSN 1580-2949
MTAEC9, 56(4)365(2022)

MECHANICAL PROPERTIES OF RC BEAMS WITH AFRP SHEETS UNDER A SUSTAINED LOAD

MEHANSKE LASTNOSTI BETONSKEGA NOSILCA OJAČANEGA S PLETIVOM AFRP POD STALNO OBREMENITVIJO

R. Mohanraj[1*], S. Senthilkumar[2], P. Padmapoorani[2]

[1]Civil Engineering, Excel Engineering College, NH544 Salem Main Road, Komarapalayam, Namakkal, Tamilnadu 637303, India
[2]Civil Engineering, KSR College of Engineering, KSR Kalvi Nilayam, Thiruchengode, Namakkal, Tamilnadu 637215, India

Prejem rokopisa – received: 2022-04-22; sprejem za objavo – accepted for publication: 2022-05-16

doi:10.17222/mit.2022.481

In this research, an attempt was made to find the permeability of an RC beam with AFRP by making use of the hydraulic conductivity test and a double-ring infiltrometer. Based on the state-of-the-art methodology, three different AFRP samples, Kelvar 29, Kelvar 49 and Kelvar 149, were considered as the laminates to prevent the deflection of the beams. Accelerated corrosion was carried out using impressed current, and induced corrosion was calculated using the galvanostatic method. In this project, nine RCC beams were strengthened with aramid FRP sheets. Novel results were obtained using three different layers and three different patterns of AFRP sheets. Experimental investigation showed that the mechanical properties of the reinforced concrete beams were enhanced (by 10 %) with Kelvar 149. The durability and corrosion resistance of concrete were achieved due to the increased number of layers of the AFRP sheet. The entire research shows that three layers of Kelvar 149 allow better performance of the concrete specimens. No other results based on the abrasion resistance and hydraulic conductivity of beams with AFRP laminates are available in the literature.

Keywords: aramid fiber reinforced polymer, kelvar laminates, hydraulic conductivity test, reinforcement corrosion

V raziskavi so avtorji na začetku posvetili pozornost ugotavljanju prepustnosti (permeabilnosti) ojačanega betonskega nosilca (RC), ki so ga pred tem ojačali s polimernimi vlakni iz Aramida (AFRP; angl.: Aramid Fiber Reinforced Polymer). Preizkuse prepustnosti so izvajali s hidravličnimi testi prevodnosti in infiltrometrom z dvojnim obročem. Za preiskave so uporabili tri različne danes najnaprednejše vzorce AFRP in sicer Kelvar 29, Kelvar 49 in Kelvar 149 kot laminate za rešitev povečanja odpornosti nosilca proti zvijanju. Izvajali so tudi pospešene teste korozije z njihovim obremenjevanjem z električno napetostjo in tokom ter na njihovi osnovi izračunali inducirano korozijo z uporabo galvanostatične metode. Za raziskavo so uporabili devet RCC nosilcev ojačanih z AFRP. Nov pristop in rezultat so dosegli s tremi različnimi plastmi in tremi različnimi vzorci pletenja laminatnih polnil AFRP (pletenih tankih plošč). Eksperimentalne raziskave so pokazale, da so se mehanske lastnosti ojačanih betonskih nosilcev izboljšale za 100 % pri uporabi laminatov iz Kevlarja 149. Trajnost in odpornost betona proti koroziji se je povečala s povečevanjem števila plasti laminata AFRP. Raziskava je pokazala, da tri plasti laminata iz Kevlarja 149 močno izboljšajo lastnosti betonskih vzorcev. V literaturi avtorji niso našli podatkov o abrazijski odpornosti in hidravlični prevodnosti betonskih nosilcev ojačanih z laminati AFRP.

Ključne besede: aramidna vlakna, polimer, kelvar, test hidravlične prevodnosti, korozija

1 INTRODUCTION

The durability of concrete is a potential problem governed by several factors such as low compressive strength, high chance of clogging and low abrasion resistance under dynamic loading.[1] The use of FRP composites to strengthen reinforced-cement-concrete (RCC) beams is becoming increasingly common.[2] For many reasons, aramid fiber reinforced polymer (AFRP) is more convenient than steel. The usage of advanced fiber reinforced polymer/plastics (FRP) composites for reinforced concrete beams has grown in popularity in recent years.[3] This is because the structure:

- may require alteration due to aging,
- corrosion in steel induced by exposure to a hostile environment may cause it to deteriorate,
- may require strengthening to withstand accidental loads such as earthquakes, etc.[4]

Flexural failure and shear failure are the two important failure modes in any flexural member. The former is a ductile failure and the latter is a brittle failure.[5,6] A ductile failure distributes the stress and alerts the occupants, whereas a brittle collapse occurs suddenly and is consequently disastrous.[7,8] To strengthen flexural members against a brittle failure, different strengthening techniques/materials are commonly adopted.

FRP is one of the strengthening materials recommended, instead of steel, for several reasons.[9] Compared to steel, the FRP material has higher ultimate strength and lower density, as well as being easier to install and requiring no interim support until it reaches its full strength.[10] This material can be easily shaped into complex shapes and cut to the desired length on the job site. Fibers are normally classified as GFRP, CFRP and AFRP.[11,12] From a structural standpoint, FRP is primarily used in two areas. The first is the use of FRP

*Corresponding author's e-mail:
rsrirammohan@gmail.com

sheets/plates to reinforce structural components using externally applied FRP.[13] The focus here is on potential enhancement of the toughness and durability provided by synthetic macro-fibers, which helps us to develop new applications of AFRP.[14] Steel has a stronger ultimate strength but a lower density than aramid FRP, as well as being easier to install and requiring no interim support until it reaches its full strength.

Among the above fiber polymers, aramid fiber reinforced polymer is interesting and challenging when used for improving mechanical and corrosion resistance of concrete specimens.[15–17] However, expanding its use beyond the lime-based concrete in historical buildings to commercially available goods would help us to better comprehend its potential in its current applications. Therefore, in this research, aramid fiber reinforced polymer was used for laminated sheets in fresh and hardened concrete to evaluate the durability and corrosion resistance of concrete.

2 EXPERIMENTAL PART

2.1 Materials

Portland Pozzolana cement of 53 grade was used in this investigation. The cement was tested as per IS 2720 Part-3. Fine aggregate (FA) for the experimental examination was obtained locally and used in accordance with IS: 383-1970. Coarse aggregates are manufactured from stones by breaking them. A 20 mm aggregate (max.), locally available for our work, suited the nature of our operation.[18] Coarse aggregates (CAs) were examined in accordance with the Indian Standard Specifications, IS:2386-1963. Steel bars of grade Fe 415 (HYSD) with 6-mm, 8-mm and 12-mm diameters were used. 12-mm-diameter bars were utilized as the tension reinforcement, while 8-mm-diameter bars were employed as hanger bars. 6-mm-diameter bars were utilized as shear stirrups. The cement, sand and coarse-aggregate properties are displayed in **Table 1**. Aramid fibers, known under their trademark name Kevlar, have unique and beneficial properties. The brand name Kevlar is owned by DuPont.[19] Poly-paraphenylene terephthalamide was the chemical name for Kevlar when it was first developed in the 1960s.[20] Kevlar has idiosyncratic properties such as excellent impact resistance and low density.[21] The three different patterns of the AFRP sheets used in this study and their properties are listed in **Table 2**. Kelvar 29 has a knitted mesh reinforcement shape, Kelvar 49 has a chicken mesh reinforcement shape, and Kelvar 149 has a honeycomb reinforcement shape, shown in **Figures 1a** to **1c**.

Table 1: Physical properties of the materials

Physical property	Cement	FA	CA
Specific gravity	3.13	2.66	2.76
Fineness modulus (%)	2.32	3.71	7.42
Water absorption (%)	–	0.6	0.5
Consistency (%)	30.5	–	–
Initial setting time (min)	34	–	–
Final setting time (h)	10	–	–

Table 2: Properties of different AFRP sheets

AFRP patterns	Density (g/cm^3)	Tensile strength (MPa)	Modulus (GPa)
Kelvar 29	1.44	2920	83
Kelvar 49	1.44	3600	124
Kelvar 149	1.47	3450	174

2.2 Hydraulic conductivity

This is a property that permits fluids to flow through interconnecting voids, and can be measured in terms of permeability (k) and infiltration (I). Here, permeability was measured with a constant head permeameter, and infiltration with a double ring infiltrometer.

2.3 Abrasion-resistance test methods

These test methods were used to determine the raveling resistance (ASTM C1747) and surface wearing (ASTM C944). A Los Angeles abrasion-test apparatus was used to determine the toughness and raveling index, and a rotating-cutter drill press was used to determine the disintegration and degradation. Cylindrical samples with a diameter and height of 100 mm were used in these tests.

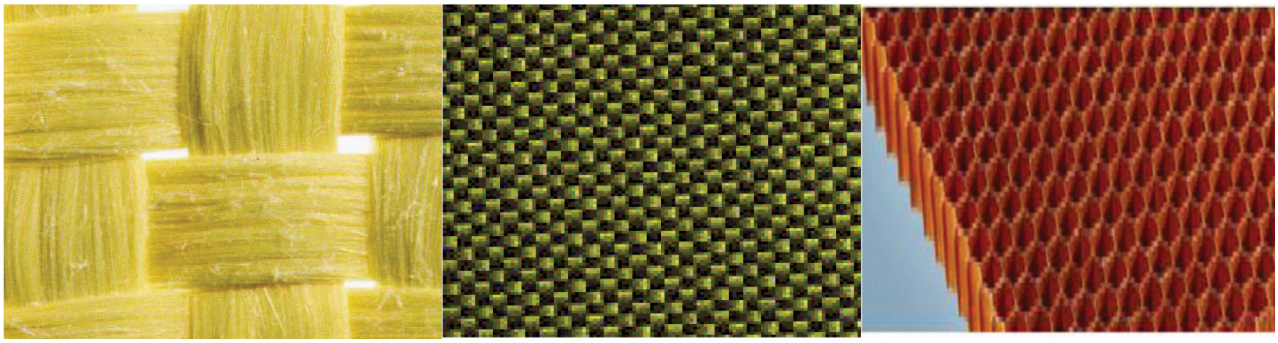

Figure 1: Kevlar patterns: a) Kelvar 29, b) Kelvar 49, c) Kelvar 149

2.4 Flow index

The flow index is a direct measure of the workability of a freshly prepared concrete mix.[22] The effects of the change in the aggregate size and change in the fiber length on the consistency of the flow percentage are demonstrated in detail in **Table 3**. The consistency in the flow percentage of a fresh concrete mix was inversely proportional to the aggregate size, i.e., the flow index increased with a decrease in the aggregate size. The flow index of a given fresh concrete mix was also inversely proportional to the fiber length, i.e., the flow index decreased with an increase in the fiber length. The elevated values of the flow index observed for the aramid-fiber-reinforced polymer mix were high due to the addition of a viscosity-modifying agent: Eucoplacant-721.

Table 3: Flow index values

Mix ID	Conventional	Concrete with AFRP
Flow (%)	98	111

3 RESULT AND DISCUSSION

3.1 Compressive tests on concrete cubes

As per IS 10262:2009,[12] concrete mix proportions for M40 grade were designed. This ratio determined the design procedure using the properties of the materials. A mix ratio of 1 : 1.01 : 2.92 (cement : FA : CA) was obtained based on the mix design method.[23–25] The water-cement ratio for this design was 0.41. The compressive test results are shown in **Table 4**.

Table 4: Compressive tests on concrete cubes

Test specimen	Grade of concrete cube	Compressive strength after 28 d (N/mm^2)	Average compressive strength (N/mm^2)
1	M_{40}	43.67	43.40
2	M_{40}	42.38	
3	M_{40}	44.16	

3.2 Hydraulic conductivity

3.2.1 Permeability

Permeability (k) of cylindrical samples was tested, as shown in **Figure 2a,** using Equation (1). The samples were subjected to a vacuum wash before testing to get more accurate results.

$$k = \frac{QL}{Ah\Delta t} \tag{1}$$

Here, Q is the volume of discharge (m^3), L is the specimen length (0.1 m), A is the cross-sectional area of the cylinder (m^2), h is the water head (m), and Δt is the time interval (s).

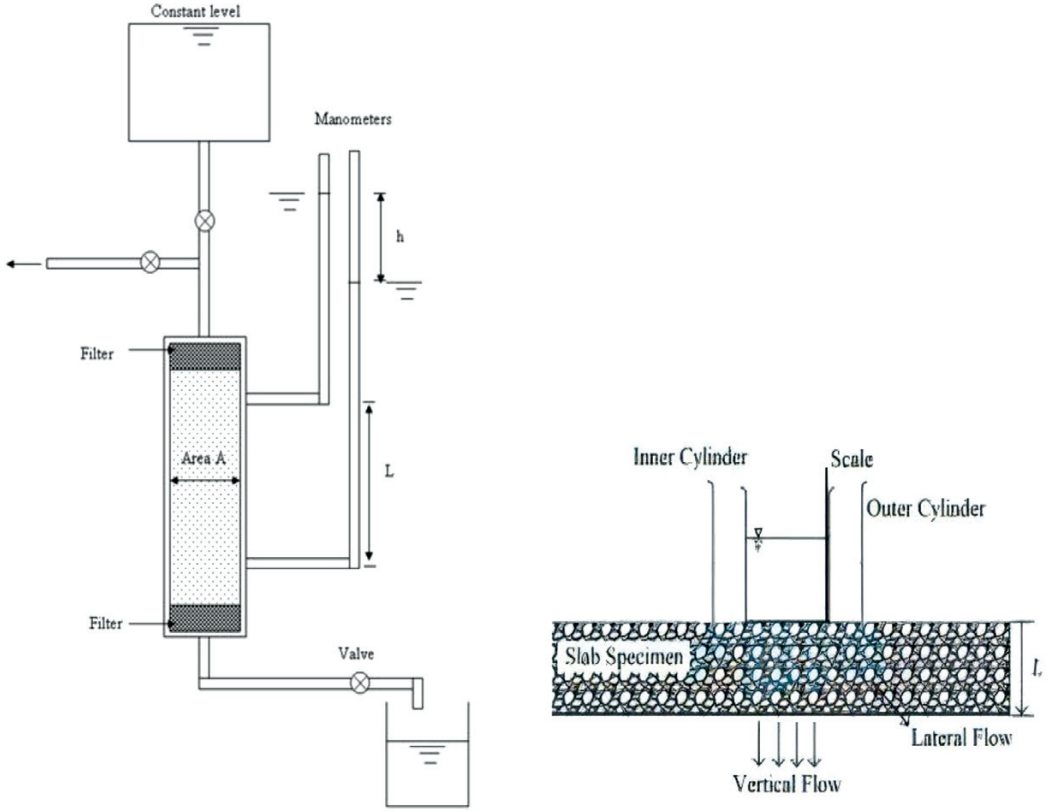

Figure 2: Test set-up for measuring permeability (k) and infiltration rate (I): a) constant head permeameter, b) double ring infiltrometer

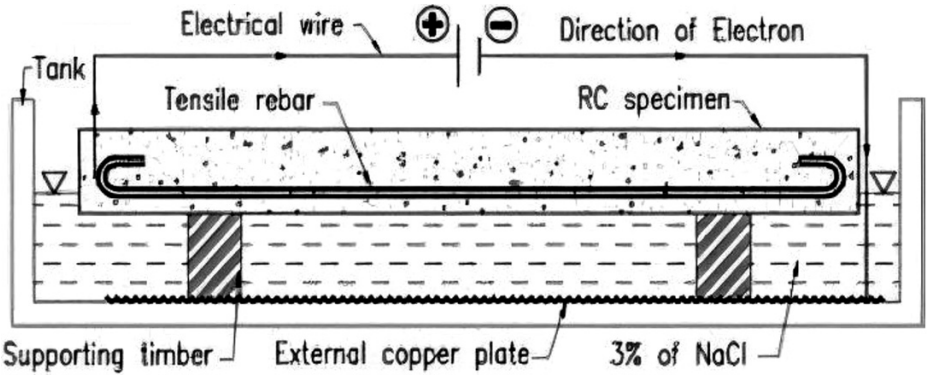

Figure 3: Accelerated corrosion set-up

Table 5: Hydraulic conductivity test result

Concrete mix	*k*/(cm/s)	Coefficient of variance (%)	*I*/(cm/s)	Coefficient of variance (%)
Conventional	1.31	23.1	0.30	2.3
AFRP concrete	1.12	10.0	0.32	14.6

3.2.2 Infiltration

Infiltration *(I)* testing required two cylindrical rings, one with a diameter of 300 mm (the inner cylinder) and the other with a diameter of 600 mm (the outer cylinder) placed over the slab specimen with a length of 1000 mm and depth of 100 mm as shown in **Figure 2b**. Initially, water was poured into the cylinder and then the rapidity of infiltration of the water was noted using the scale attached, determining the time and depth of the infiltration into the slab specimen using Equation (2). The values of the infiltration rate are given in **Table 5**.

$$I = \frac{4V}{\pi D_i^2 \Delta t} \tag{2}$$

Here, V is the volume (m^3) of water added in time Δt, D_i is the diameter of the inner cylinder and Δt is the time interval (s).

3.3 Accelerated corrosion test and calculation

Corrosion of the reinforced steel was carried out using the impressed current technique. Beams of 1 m in length and with a cross-section of 150 mm × 200 mm were cast for each optimum AFRP mix and the control mix (the total of 10 samples). The tension reinforcement was wound with wires at two points so that uniform corrosion was initiated in the rebars.[26] Only the corrosion of the tension reinforcement was considered for the study. The test set-up for accelerated corrosion is shown in **Figure 3**.

The impressed current technique, applying direct current constantly to the steel embedded in the concrete for a short period, allowed accelerated corrosion, which was later observed on the steel after inducing electrolytes in the concrete. The rate of corrosion was accelerated through the concrete with the help of electrolytes (3 % of sodium chloride solution). For the provided power supply, the induced corrosion was determined using Faraday's law. If the source current was increased, the rate of accelerated corrosion was also increased. The amount of weight loss of steel was calculated using a gravimetric test, determining the weight loss during corrosion. The source which consisted of an anode and a cathode was connected to the steel bars and the counter electrode – stainless steel plates, respectively. The reinforcements fabricated for the corrosion acceleration test are shown in **Figure 4**.

Current readings were noted every hour using a multimeter and the average current reading was used in the calculation as the applied current (I_{app}). The beams were kept in the acceleration corrosion process for 120 h. Lead wires were connected at two points of each tension reinforcement to ensure uniform corrosion throughout the beam. Only the corrosion of the tension reinforcement was considered.

After generating corrosion on the beams, the bars were retrieved from the beams by fracturing the concrete and measured using the gravimetric test to determine the average loss of steel due to induced corrosion. To remove any rust products, the bars were cleaned using chemical cleaning and weighed to calculate the steel net weight.

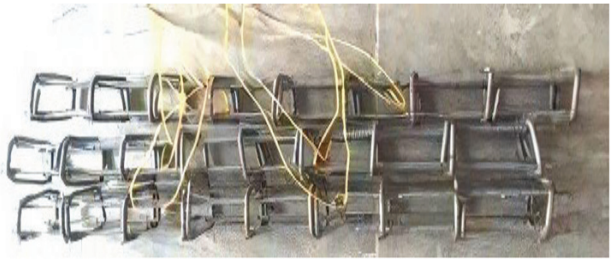

Figure 4: Reinforcement for the corrosion acceleration test

Table 6: Accelerated corrosion test results

Beam ID	No. of Layer	Average I_{app} (A)	Initial weight (g)	Final weight (g)	Actual weight loss (g)	Theoretical weight loss (g)	Actual weight loss (%)
Conventional	–	1.02	2823	2703	120	126.56	4.22
B FRP K29	1	1.19	2858	2665	193	150.11	5.06
B FRP K29	2	1.57	2836	2657	179	97.84	6.24
B FRP K29	3	0.81	2860	2782	78	102.14	2.80
B FRP K49	1	0.73	2835	2767	68	89.60	2.40
B FRP K49	2	0.75	2808	2733	75	95.05	2.67
B FRP K49	3	0.76	2841	2764	77	95.67	2.71
B FRP K149	1	0.77	2853	2775	78	93.63	2.77
B FRP K149	2	0.87	2851	2766	85	107.69	3.02
B FRP K149	3	0.87	2861	2775	86	107.38	3.07

Following ASTM G-1-90 (ASTM, 1990), the corrosion test specimens were prepared, cleaned and evaluated.

For the current capacity of the circuit, the current applied to the fiber specimens was found to be lower than that of the control specimens.

From **Table 6**, it can be understood that the conductance of the fiber specimens was lower compared to the control specimens, which in turn indicates higher porosity of the control specimens. Thus, it can be concluded that the fiber has a higher corrosion resistance and it can effectively be used in an aggressive environment. The mass loss percentages of the fiber specimens were found to be lower than that of the control mix without fiber.

In accordance with Faraday's law, the theoretical mass of rust (M_{th}) was determined with Equation (3):

$$M_{th} = \frac{WI_{app}T}{F} \tag{3}$$

where M_{th} is the theoretical mass of rust or mass loss (g), W is the equivalent weight of steel (27.925 g), I_{app} is the current applied (A), T is the period of induced corrosion (s) and F is Faraday's constant (96487 As).

After the corrosion test, the specimens and rebars were extracted by breaking the concrete. In accordance with the gravimetric test (ASTM G1), the actual mass (M_{ac}) of rust was calculated with Equation (4):

$$M_{ac} = \frac{W_i - W_f}{\pi DL} \tag{4}$$

where W_i is the initial weight of the rebar, W_f is the weight of the rebar after corrosion, D is the diameter of the rebar and L is the length of the rebar.

Assuming that the actual and theoretical mass of rust were equal (i.e., $I_{corr} = I_{app}$) and by equating M_{ac} and M_{th}, the equivalent corrosion current (I_{corr}) was calculated with Equation (5):

$$I_{corr} = \frac{(W_i - W_f)F}{WT} \tag{5}$$

Where,

W_i – Initial Weight

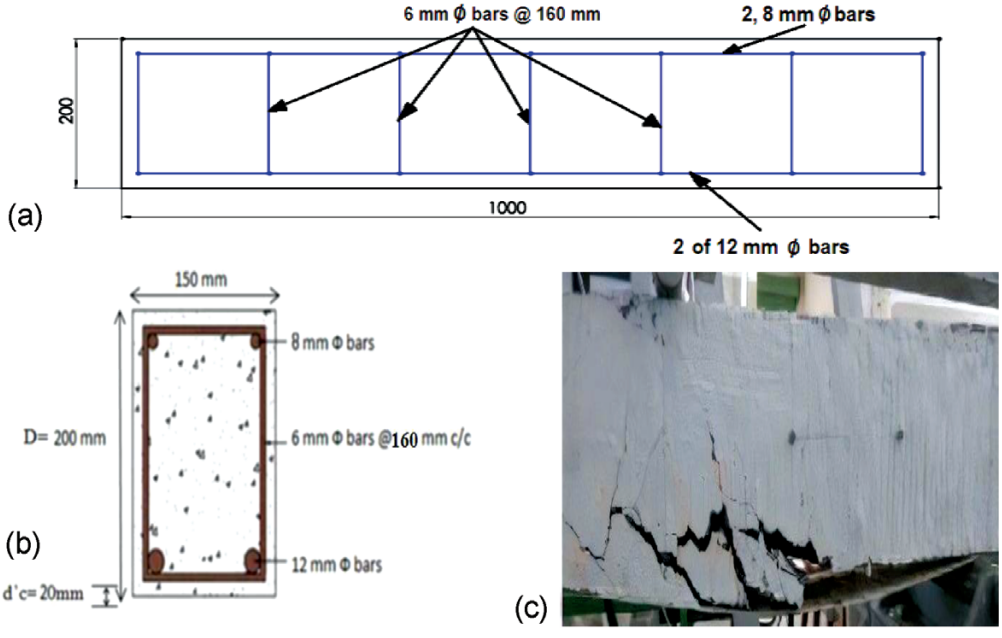

Figure 5: a) Reinforcement details of a beam, b) cross-section of a beam, c) beam failure

W_f – Final Weight
F – Faraday Constant
W – Equivalent weight of steel
T – The period of induced corrosion

The percentage weight loss (P) was calculated with Equation (6):

$$P = \frac{W_i - W_f}{W_i} \times 100\ \% \quad (6)$$

3.4 Tests with beams

3.4.1 Experimental work

This experimental task entailed casting M40 reinforced concrete (RC) beams with cross-sectional dimensions of (150 × 200 × 1000) mm. Two of 12 mm diameter were placed at the base, at a 160-mm center-to-center distance, with the top having ϕ 2–8 mm and ϕ 6 mm vertical stirrups.[27,28] Single, double and triple-layer AFRP were three alternative patterns and layer combinations used to strengthen the beams utilizing AFRP sheets.[29] Totally, ten reinforced concrete beams were cast and kept in water for curing for 28 d.

3.4.2 Experimental set-up

All the specimens were put through their paces in the loading frame, and the deflection was measured with a linear variable differential transformer (LVDT) machine.[30] They were subjected to the same testing procedures. After the 28-d cure time, the beams had three layers and three patterns, there were also conventional beams. The load arrangements for evaluating all sets of beams included two-point loading, and reinforcement details are shown in **Figures 5a** and **5b**. The testing of a beam is shown in **Figure 5c**.

3.4.3 Beam specification

The length of a beam was 1000 mm, its span was 800 mm, its width was 150 mm, its depth was 200 mm and the numbers of layers were specified as shown in **Table 6**.

3.4.4 Beam results

The performance of the specimens under load was noted. It was discovered that, with the growing load, the cracks additionally began to show up, constantly increasing. A few cracks went throughout the beam. The crack pattern was also noticed. The values of load and deflection for various volumes of Kelvar 29 and conventional concrete were examined and listed in **Table 7**.

Table 7: Deflection of conventional concrete and Kelvar 29

Load (kN)	Deflection (mm)			
	Conventional concrete	Single layer	Double layer	Triple layer
0	0	0	0	0
50	0.112	0.090	0.050	0.025
100	1.730	1.001	0.800	0.475
150	4.192	3.002	2.182	1.290

It is seen that the bend followed a straight pattern until the first break load. With the additional increase in load, numerous cracks were formed, the number of which increased as a certain load was reached. The outcomes obtained show improved primary conduct, like that of FRP. If the number of layers increased, the deflection against the load decreased.

The values of load and deflection for various volumes of Kelvar 49 and Kelvar 149 were analyzed, and their properties are listed in **Table 8** and **Table 9**. It is perceived that the bend followed a straight pattern until the first break load. With the additional increase in load, numerous cracks were formed, the number of which increased as a certain load was reached.

Table 8: Deflection of Kelvar 49

Load (kN)	Deflection (mm)		
	Single layer	Double layer	Triple layer
0	0	0	0
50	0.0925	0.066	0.039
100	1.115	0.978	0.575
150	3.125	2.264	1.390

Table 9: Deflection of Kelvar 149

Load (kN)	Deflection (mm)		
	Single layer	Double layer	Triple layer
0	0	0	0
25	0.030	0.017	0.005
50	0.046	0.037	0.015
75	0.280	0.230	0.130
100	0.560	0.548	0.292
125	1.890	0.880	0.520
150	1.625	1.264	0.800

4 CONCLUSIONS

The outcomes obtained show an increase in the strength with the increasing the number of layers. The deflection against load was lower for three-layer Kelvar 49 and 149. The physical properties of the materials, hydraulic conductivity, flow index, compressive strength of a concrete cube were tested on the beams and the results obtained are presented.

The aggregate size and fiber length were inversely linked to the consistency in the flow percentage of a fresh concrete mix. The increase in the flow index of aramid concrete compared to the conventional mixes was due to the addition of a viscosity modifying agent. The addition of macro-synthetic fibers reduced the permeability and infiltration rate of the test samples. This was observed to be most significant for a high dosage of long fibers. The infiltration rate was about 5 times lower compared to the permeability values for the other mixtures.

Concrete mixes containing fiber showed a higher value of compressive strength than the conventional concrete. The maximum increase in the compressive strength of 22.08 % was obtained for the Kelvar 149 con-

crete. Concrete mixes containing fiber showed lower values of water absorption than the conventional concrete, hence the plugging of pores was better than in the conventional concrete. The corrosion resistance of the AFRP concrete specimens was found to be higher than that of the conventional concrete specimens.

The weight loss percentages were higher for the control specimens when compared with the fiber concrete specimens. Based on performance, a triple layer is better than a double layer or a single layer. It was also observed that the influence of the fiber length was not as substantial as that of the aggregate size. The effect of the sudden release technique should be further examined. Additional research is needed for aramid fiber-reinforced polymer members with different types of concrete (i.e., lightweight concrete, high-performance concrete, etc.).

Acknowledgements

This research is supported by Excel Engineering College and KSR College of Engineering. The author would like to thank M/s. Modern Builders Pvt. Ltd. for providing the strands for this research. The author would also like to thank a number of individuals at the College Campus for their contribution to this research.

Declarations of interest

My co-author and I do not have any interests that might be interpreted as influencing the research. "Conflict of interest: none".

5 REFERENCES

[1] F. Abed, H. El-Chabib, M. Al Hamaydeh, Shear characteristics of GFRP-reinforced concrete deep beams without web reinforcement, Journal of Reinforced Plastics and Composites, 31 (**2012**) 16, 1063–1073, doi:10.1177/0731684412450350

[2] M. A. Dar, N. Subramanian, A. R. Dar, A. I. Rather, M. Atif, S. Syed, Strengthening of capacity deficient RC beams – An experimental approach, Structural Engineering and Mechanics, South Korea, 70 (**2019**) 3, 303–310, doi:10.12989/sem.2019.70.3.303

[3] M. Amer, M. Ibrahim, Sh. Mahmood, Finite element modeling of reinforced concrete beams strengthened with F laminates, European Journal of Scientific Research, 30 (**2009**) 4, 526–541

[4] N. K. Banjara, K. Ramanjaneyulu, Experimental and numerical investigations on the performance evaluation of shear deficient and GFRP strengthened reinforced concrete beams, Construction and Building Materials, 137 (**2017**), 520–534, doi:10.1016/j.conbuildmat.2017.01.089

[5] V. Behnam, N. Shami, Self-compacting light-weight concrete; mix design and proportions, Struct. Eng. Mech., 58 (**2016**) 1, 143–161, doi:10.12989/sem.2016.58.1.143

[6] C. Pellegrino, C. Modena, Fiber-Reinforced Polymer Shear Strengthening of Reinforced Concrete Beams: Experimental Study and Analytical Modeling, ACI Structural Journal, 103 (**2006**) 5, 720–728

[7] J. F. Chen, T. G. Teng, Shear capacity of FRP-strengthened RC beams: FRP debonding, Construction and Building Materials, 17 (**2003**) 1, 27–41, doi:10.1016/S0950-0618(02)00091-0

[8] A. Deifalla, A. Awad, M. Elgarhy, Effectiveness of externally bonded CFRP strips for strengthening flanged beams under torsion: An experimental study, Engineering Structures, 56 (**2013**), 2065–2075, doi:10.1016/j.engstruct.2013.08.027

[9] N. F. Grace, G. A. Sayed, A. K. Soliman, K. R. Saleh, Strengthening reinforced concrete beams using fiber reinforced polymer (FRP) laminates, ACI Structural Journal, 188 (**1999**) 8, 865–874, doi:10.14359/741

[10] H. D. Tahar, A. Boussad, R. Abderezak, B. Rabia, A. Fazilay, A. Belkacem, Flexural behaviour of steel beams reinforced by carbon fibre reinforced polymer: Experimental and numerical study, Structural Engineering and Mechanics, South Korea, 72 (**2019**) 4, 409–419, doi:10.12989/sem.2019.72.4.409

[11] M. R. Islam, M. A. Mansur, M. Maalej, Shear strengthening of RC deep beams using externally bonded FRP systems, Cement and Concrete Composites, 27 (**2005**) 3, 413–420, doi:10.1016/j.cemconcomp.2004.04.002

[12] IS 10262:2009, Concrete Mix Proportioning – Guidelines. Bureau of Indian Standards, New Delhi

[13] O. Kayali, Fly ash lightweight aggregates in high performance concrete, Construction and Building Materials, 22 (**2008**) 12, 2393–2399, doi:10.1016/j.conbuildmat.2007.09.001

[14] R. S. Kareem, A. Al-Mohammedi, C. N. Dang, J. R. Martí-Vargas, W. M. Hale, Bond model of 15.2-mm strand with consideration of concrete creep and shrinkage, Mag. Concr. Res., 72 (**2019**) 15, 799–810, doi:10.1680/jmacr.18.00506

[15] K.-H. Yang, K.-H. Lee, H.-S. Yoon, Flexural tests on two-span unbonded post-tensioned lightweight concrete beams, Structural Engineering and Mechanics, South Korea, 72 (**2019**) 5, 631–642, doi:10.12989/sem.2019.72.5.631

[16] A. M. Kulkarni, D. Datta, Probabilistic analysis of RC beams according to IS456: 2000 in limit state of collapse, Struct. Eng. Mech, 71 (**2019**) 2, 165–173, doi:10.12989/sem.2019.71.2.165

[17] A. Kumari, A. N. Nayak, Strengthening of shear deficient RC deep beams using GFRP sheets and mechanical anchors, Canadian Journal of Civil Engineering, 48 (**2019**) 1, doi:10.1139/cjce-2019-0333

[18] A. Kumar, A. K. Chaubey, S. Vishwakarma, S. Fic, D. Barnat-Hunek, Transient response of rhombic laminates, Structural Engineering and Mechanics, 70 (**2019**) 5, 551–562, doi:10.12989/sem.2019.70.5.551

[19] M. S. Manideep, A. K. Chaubey, M. S. R. Rao, Experimental investigation on flexural behaviour of sandwich slabs with and without concealed beams, In: International Conference on Advances in Civil Engineering, 21 (**2019**) 23

[20] M. R. Mohammadizadeh, M. J. Fadaee, H. R. Ronagh, Improving torsional behaviour of reinforced concrete beams strengthened with carbon fibre reinforced polymer composite, Iranian Polymer Journal, 18 (**2009**) 4, 315–327

[21] J. H. Mun, Y. H. Yang, Flexural behaviour of externally post-tensioned two-span lightweight concrete beams, Magazine of Concrete Research, 71 (**2019**) 22, 1193–1203, doi:10.1680/jmacr.17.00533

[22] F. N. Grace, G. Abdel-Sayed, F. R. Wael, Strengthening of concrete beams using innovative ductile fiber-reinforced polymer fabric, ACI Structural Journal, 99 (**2002**) 5, 692–700, doi:10.14359/12309

[23] A. N. Siddiqui, Experimental investigation of RC beams strengthened with externally bonded FRP composites, Latin American Journal of Solids and Structures, 6 (**2009**) 4, 343–362

[24] Y. Obaidat, S. Heyden, O. Dahlblom, G. Abu-Farsakh, Y. Abdel-Jawad, Retrofitting of reinforced concrete beams using composite laminates, Construction and Building Materials, 25 (**2011**) 2, 591–597, doi:10.1016/j.conbuildmat.2010.06.082

[25] R. Liu, Y. Yang, Analysis on damage of RC frames retrofitted with buckling-restrained braces based on estimation of damage index, Structural Engineering and Mechanics, South Korea, 70 (**2019**) 6, 781–791, doi:10.12989/sem.2019.70.6.781

[26] U. M. Rameshkumar, D. B. Kulkarni, Flexural behavioral study on RC beam with externally bonded aramid fiber reinforced polymer,

International Journal of Research in Engineering and Technology, 03 (**2014**) 7, 316–321, doi:10.15623/IJRET.2014.0307054

[27] T. Roik, A. Rashedi, T. Khanam, A. Chaubey, G. Balaganesan, S. Ali, Structure and properties of new antifriction composites based on tool steel grinding waste, Sustainability, 13 (**2021**) 16, 8823, doi:10.3390/su13168823

[28] S. Barakat, S. Altoubat, M. Leblouba, E. Al Burai, Behavioral trends of shear strengthened reinforced concrete beams with externally bonded fiber-reinforced polymer, Structural Engineering and Mechanics, South Korea, 69 (**2020**), 579–589, doi:10.12989/sem.2020.76.1.067

[29] M. C. Sundarraja, S. Rajamohan, Strengthening of RC beams in shear using GFRP inclined strips – An experimental study, Construction and Building Materials, 23 (**2009**) 2, 856–864, doi:10.1016/j.conbuildmat.2008.04.008

[30] L. Wang, Z. He, X. Cai, Characterization of pozzolanic reaction and its effect on the CSH Gel in fly ash-cement paste, Journal of Wuhan University of Technology-Mater. Sci. Ed., 26 (**2011**) 2, 319–324, doi:10.1007/s11595-011-0222-4